Received: 26 November 2018 | Revised: 29 January 2019 | Accepted: 31 January 2019

DOI: 10.1002/rcm.8406

RESEARCH ARTICLE

WILEY Rapid Communications in Mass Spectrometry

Matrix-assisted laser desorption/ionization time-of-flight mass spectrometry analysis for characterization of lignin oligomers using cationization techniques and 2,5-dihydroxyacetophenone (DHAP) matrix

Amber S. Bowman | Shardrack O. Asare | Bert C. Lynn

Department of Chemistry, University of Kentucky, Lexington, KY 40506, USA

Correspondence
Bert C. Lynn, Department of Chemistry, UK Mass Spectrometry Facility, University of Kentucky, A053 ASTeCC Building, Lexington, KY 40506-0286, USA.
Email: bclynn2@uky.edu

Funding information
National Science Foundation, Grant/Award Number: OIA 1632854

Rationale: Effective analytical techniques are needed to characterize lignin products for the generation of renewable carbon sources. Application of matrix-assisted laser desorption/ionization (MALDI) in lignin analysis is limited because of poor ionization efficiency. In this study, we explored the potential of cationization along with a 2,5-dihydroxyacetophenone (DHAP) matrix to characterize model lignin oligomers.

Methods: Synthesized lignin oligomers were analyzed using the developed MALDI method. Two matrix systems, DHAP and α-cyano-4-hydroxycinnamic acid (CHCA), and three cations (lithium, sodium, silver) were evaluated using a Bruker UltraFlextreme time-of-flight mass spectrometer. Instrumental parameters, cation concentration, matrix, sample concentrations, and sample spotting protocols were optimized for improved results.

Results: The DHAP/Li^+ combination was effective for dimer analysis as lithium adducts. Spectra from DHP and ferric chloride oligomers showed improved signal intensities up to decamers (*m/z* 1823 for the $FeCl_3$ system) and provided insights into differences in the oligomerization mechanism. Spectra from a mixed DHP oligomer system containing H, G, and S units showed contributions from all monolignols within an oligomer level (e.g. tetramer level).

Conclusions: The DHAP/Li^+ method presented in this work shows promise to be an effective analytical tool for lignin analysis by MALDI and may provide a tool to assess lignin break-down efforts facilitating renewable products from lignin.

1 | INTRODUCTION

Lignin is the second most abundant naturally occurring polymer and is composed of three monolignol units, coumaryl alcohol (H), coniferyl alcohol (G), and sinapyl alcohol (S). Lignin chemistry has increased in relevance for its use in biorefineries, bioplastics, and renewable sources of carbon for fine materials.[1-5] While gains have been made in lignin depolymerization chemistry, comprehensive analytical techniques are still needed to effectively characterize the resulting products.[6-8]

Matrix-assisted laser desorption/ionization coupled with time-of-flight mass spectrometry (MALDI-TOF-MS) is a powerful technique that has been used to characterize synthetic polymers and proteins; however, its application in lignin analysis is limited due to the poor

ionization efficiency of lignin.[9,10] Yoshioka et al evaluated MALDI-TOF-MS using a 2,5-dihydroxybenzoic acid (DHB) matrix with trifluoroacetic acid (TFA) and nanostructured-assisted laser desorption/ionization (NALDI) to analyze dehydrogenation polymer (DHP) synthetic lignin oligomers. While both methods produced useful spectra, the NALDI spectra showed a slight signal enhancement in the mass range of *m/z* 500 to 800.[9] Yoshioka et al did not comment on the form of the ions observed (protonated vs cationized); however, the addition of TFA indicates that they were interested in protonation. Richel et al utilized an α-cyano-4-hydroxycinnamic acid/α-cyclodextrin (CHCA/CD/TFA) matrix system to analyze formic acid/acetic acid pretreated lignin from *Miscanthus* and switch grass.[10] While their spectra were dominated by matrix ions, signals attributed to lignin monomer, dimers and trimers were observed. In discussion of their MALDI spectra, they reported monolignol signals as both proton and sodium adducts below *m/z* 200. For their system, the addition of NaCl, KCl or TFA did not improve the signals observed between *m/z* 100 and 900 when using DHB or CHCA matrix systems.

De Angelis et al also studied DHP lignin oligomers using MALDI-TOF-MS and the DHB matrix. Their results indicated that protonation was observed for dimer and trimer oligomers but, for higher oligomers, cationization was a significant contributor to ionization.[11] Cation adduct formation was observed in the spectra of many lignin oligomer systems even without addition of external cations, illustrating the potential for cationization to enhance MALDI ion intensities, but finding a compatible matrix to support cationization is critical.[12]

In protein and biomolecular studies, 2,5-dihydroxyacetophenone (DHAP) was shown to be a robust crystalline MALDI matrix.[13-15] DHAP is known to produce less complex spectra with better mass resolution than some more commonly used matrices such as CHCA and DHB. In a study by Penno et al, the optimal sample preparation of several commonly used matrices with small proteins and peptides was compared and analyzed via MALDI-TOF-MS. The eight differently prepared matrices were then scored and ranked to determine the best sample preparation in a variety of categories. They observed that the DHAP matrix as a dried droplet preformed best overall and scored highest in mass resolution and signal intensity, both of which have been issues with lignin analyses previously.[12] The addition of metal salts, such as Li^+, Na^+, and K^+, to the DHAP matrix has been reported to increase analyte response in MALDI analysis.[16,17]

To extend our previous work using lithium cationization with the electrospray analysis of lignin,[18] we investigated a MALDI method using DHAP as a matrix and lithium cationization for lignin oligomers. Due to lithium's small ionic radius, charge density, and ability to coordinate to multiple oxygen atoms,[19] it was found to be superior to other cations. Nine synthesized lignin β-O-4' model dimers were analyzed by MALDI-TOF-MS. The DHAP matrix was compared with a CHCA matrix and lithium was compared with other cations where the metrics for evaluation were the presence of interfering ion signals, mass resolution and signal intensity. To further test DHAP/Li^+ MALDI, two different lignin oligomer systems were analyzed.

2 | EXPERIMENTAL

2.1 | Chemicals

Ethyl acetate (certified ACS), acetone (certified ACS), water (Optima), acetonitrile (Optima), sodium phosphate monobasic (certified ACS), sodium phosphate dibasic (certified ACS), 30% hydrogen peroxide (certified ACS) and horseradish peroxidase (Alfa Aesar J60026MC) were obtained from Fisher Scientific (Hampton, NH, USA). Ferric chloride (reagent grade), 2,5-dihydroxyacetophenone, α-cyano-4-hydroxycinnamic acid, lithium chloride, lithium acetate, sodium chloride, and silver trifluoroacetate were obtained from Sigma Aldrich (St Louis, MO, USA).

2.2 | B-O-4′ dimer synthesis

Nine model lignin dimers, H-(β-O-4′)-H, H-(β-O-4′)-G, H-(β-O-4′)-S, G-(β-O-4′)-H, G-(β-O-4′)-G, G-(β-O-4′)-S, S-(β-O-4′)-H, S-(β-O-4′)-G, and S-(β-O-4′)-S were synthesized using previously published aldol condensation reactions.[20] Stock solutions of all dimers were prepared in acetonitrile and subsequently diluted to working solutions for analysis.

2.3 | DHP oligomer synthesis

In a typical reaction, 50 mg (0.278 mmol) of the G monolignol was dissolved in 500 µL of acetone and diluted to 10 mL with 20 mM sodium phosphate buffer (pH 6.4). Then 1 mL of the G monolignol solution was transferred to an 8-mL reaction vial containing a stir bar. At $t = 0$, 0.25 mg/mL horse radish peroxidase (HRP) solution dissolved in phosphate buffer and a 0.3% hydrogen peroxide solution dissolved in the phosphate buffer were separately pumped by a two-barrel syringe pump into the stirred reaction vial at a rate of 50 µL/min for 5 min. At $t = 5$ min, the reaction mixture was extracted with 2 mL ethyl acetate. The ethyl acetate fraction was transferred to a clean vial and analyzed without further treatment.

A mixed oligomer DHP system was prepared using the same conditions as the G monolignol above except that 333 µL of each monolignol (H, G, and S at 5 mg/mL) solution were added to the reaction vial and oligomerized.

2.4 | Ferric chloride oligomer synthesis

The G monolignol (25 mg, 0.139 mmol) was dissolved in 200 µL ethanol and transferred to 5 mL distilled water with rapid stirring. A solution of $FeCl_3$ (0.216 mmol dissolved in 5 mL distilled water) was added dropwise over 60 min. The solution was stirred for an additional 60 min and quenched by transferring to 100 mL distilled water and immediately extracted twice with 50 mL ethyl acetate. The ethyl acetate extracts were combined and passed through sodium sulfate, and the ethyl acetate was removed by rotary

evaporator to produce a slightly yellow, viscous oil. A 2.5 mg/mL solution of the reaction product was prepared in acetone and analyzed without further treatment.

2.5 | MALDI instrumentation

MALDI-TOF mass spectra were acquired using an UltraFlextreme mass spectrometer (Bruker, Billerica, MA, USA) equipped with a Smartbeam 2 Nd:YAG laser (Bruker) operating at 355 nm. Spectra were acquired using FlexControl software (version 3.3, Bruker). The dimer samples were acquired in reflectron mode with a mass range of *m/z* 100–600 using the AutoXecute function in the FlexControl software, using the following parameters specified in the software: laser attenuator range, 60 to 95%; laser repetition rate, 200 Hz, large spiral target movement; evaluation package, 25 laser shots; peak evaluation (processing method parameters; s/*n* = 6, relative intensity threshold = 0, minimum intensity threshold = 0, maximum number of peaks = 300, peak width = 0.02, height = 80%; peak parameters; half-width < 0.8 Da; fuzzy control parameters; digest/peptide and signal intensity = low) and the total number of summed successful shots, 200. The fixed instrument voltages were ion source 1, 25.00 kV; ion source 2, 22.25 kV; lens, 7.00 kV; reflector, 26.45 kV; and reflector 2, 13.40 kV. Lignin oligomer samples were acquired manually with the same fixed parameters except that the mass range was extended to *m/z* 2000. All mass spectra were processed using FlexAnalysis software (version 3.3, Bruker).

2.6 | MALDI sample preparation

Four salt solutions, lithium chloride, lithium acetate, sodium chloride, and silver trifluoroacetate, were prepared at concentrations of 10 mM in water. The DHAP matrix was prepared at 6.5 mg/mL in acetonitrile and the CHCA matrix was prepared at 10 mg/mL in 10:90 water/acetonitrile with 0.1% TFA. Stock solutions of the nine dimers were used at 1 mg/mL or diluted to a working concentration of 0.2 mg/mL in acetonitrile. All salt solutions were spotted onto the stainless-steel target individually and allowed to air dry at room temperature. Next, each of the nine dimers was spotted on top of the salt spot and allowed to dry. Finally, the matrix was added to the top of each sample spot and allowed to dry. All possible combinations of the salt solutions, dimers, and matrices were spotted, dried, and analyzed (72 in total). Control spots without any salt solutions were also made for each of the nine dimers in the CHCA and DHAP matrices to ensure that all the observed analyte signals resulted from cationization. Lignin oligomers were analyzed in the same manner with LiCl as the sole cation source.

An internal standard of hexadecyltrimethylammonium bromide (HDTMA) was used for a quantitative comparison of lignin dimer cationization using lithium and sodium cation sources. A 1 μM solution of HDTMA was prepared and introduced into the experiment. The spotting technique was the same as previously stated, but the spotting order was salt solutions, HDTMA, dimers, and then matrices. Again, all possible combinations were spotted, dried, and analyzed. The same spotting technique was utilized to measure reproducibility for the H-(β-O-4′)-H, G-(β-O-4′)-G, and S-(β-O-4′)-S dimers along with the HDTMA internal standard. Each of these three dimers was spotted seven times, dried, and analyzed.

3 | RESULTS AND DISCUSSION

3.1 | MALDI-TOF-MS spectra from the CHCA matrix

All nine dimer samples were analyzed using the CHCA matrix. No signals corresponding to a protonated dimer were observed. However, relatively weak sodium adduct ions were observed for dimers containing the S monolignol. Addition of 10 mM NaCl to the CHCA matrix generated relatively weak $[M + Na^+]^+$ ions for all nine dimers. Interestingly, lithium and silver cations were not as effective when using CHCA as matrix. As a result, CHCA was abandoned as a potential matrix.

3.2 | MALDI-TOF-MS spectra from the DHAP matrix

Preliminary MALDI experiments using DHAP/cationization were quite promising. Intense cation dimer adducts were observed when the dimer stock solutions (1 mg/mL) were analyzed. Figure 1 shows the DHAP/Li^+ MALDI mass spectrum for the S-(β-O-4′)-S dimer. The lithium adduct ion peak at *m/z* 443 dominates the spectrum. Matrix and background peaks present in the spectrum were minimal. Peaks at *m/z* 153, 159 and 311 can be attributed to $[DHAP+H^+]^+$, $[DHAP +Li^+]^+$ and $[2DHAP+ Li^+]^+$, respectively, while peaks at *m/z* 242 and 284 are consistent with tetraalkylammonium contaminants from the last step in the synthesis of the dimer. The peaks observed at *m/z* 459 and 475 are consistent with sodium

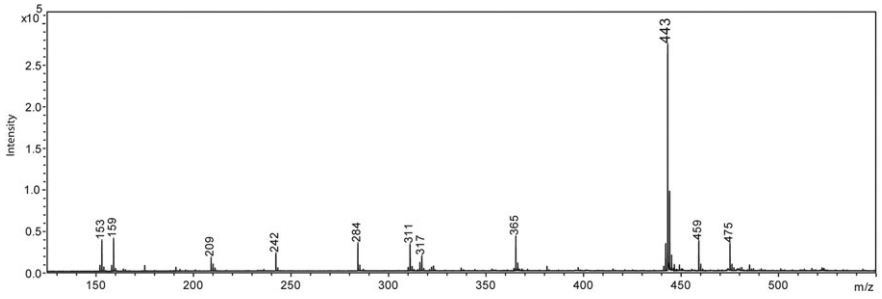

FIGURE 1 Full scan MALDI spectrum of a S-(β-O-4′)-S dimer (*m/z* 443) at a sample concentration of 1 mg/mL obtained from DHAP containing 10 mM LiCl

and potassium adducts of the dimer, respectively, possibly resulting from the matrix or glass vessels used in the synthesis, purification, and storage or from the MALDI target. Regardless of their origin, the presence of these sodium and potassium adducts and the absence of a signal from a protonated adduct reinforce our hypothesis that protonation of β-O-4′ dimers is a low probability event compared with cationization.

In an attempt to remove analyst bias, we used the AutoXecute function in FlexControl to acquire all the dimer-cation MALDI data in an unsupervised manner. The AutoXecute function operates in an iterative way to interrogate sample spots. In a typical experiment, working from a sample list, the stepper motor moves the target to position the selected spot under the laser beam, a laser attenuator value within the predetermine range is assigned, and the laser fires 25 times to produce a summed spectrum. The summed spectrum is evaluated by a fuzzy logic algorithm using mass resolution and signal intensity as metrics. If the summed spectrum does not meet the minimum criteria, the spectrum is rejected, the target is moved using a predefined pattern and the laser power is increased or decreased depending on the fuzzy logic output. This process is continued until the 25 shot summed spectrum passes the minimum criteria. The summed spectrum is written to the sum buffer, and a second 25 shot summed spectrum is acquired. The process continues until 200 shots are summed. This automated, unsupervised acquisition was used for all the dimer-cation MALDI spectra.

The calculated and observed *m/z* values for each of the cation sources with each of nine dimers are shown in Table 1. At high analyte concentrations, all cations evaluated resulted in detectable adducts.

The H-(β-O-4′)-S dimer was used as a model compound for cationization comparison purposes, and its mass spectra are shown in Figure 2. These MALDI cation adduct spectra are fairly complex

TABLE 1 MALDI full scan mass spectral data for all cationized dimers

Dimer	Structure	MW	$[M + Li]^+$ *m/z*	$[M + Na]^+$ *m/z*	$[M + Ag]^+$ *m/z*
H-(β-O-4′)-H	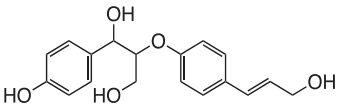	316	323	339	423
H-(β-O-4′)-G	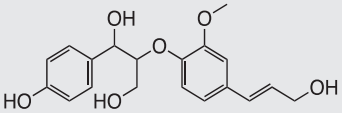	346	353	369	453
H-(β-O-4′)-S	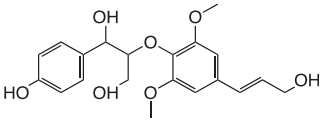	376	383	399	483
G-(β-O-4′)-H	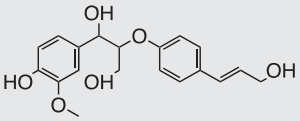	346	353	369	453
G-(β-O-4′)-G	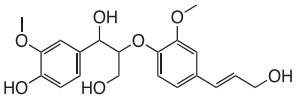	376	383	399	483
G-(β-O-4′)-S	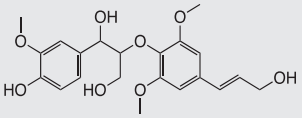	406	413	429	513
S-(β-O-4′)-H	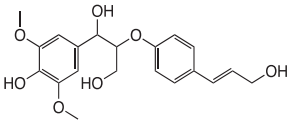	376	383	399	483
S-(β-O-4′)-G	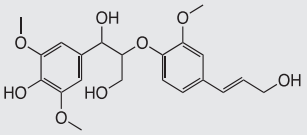	406	413	429	513
S-(β-O-4′)-S	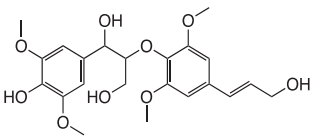	436	443	459	543

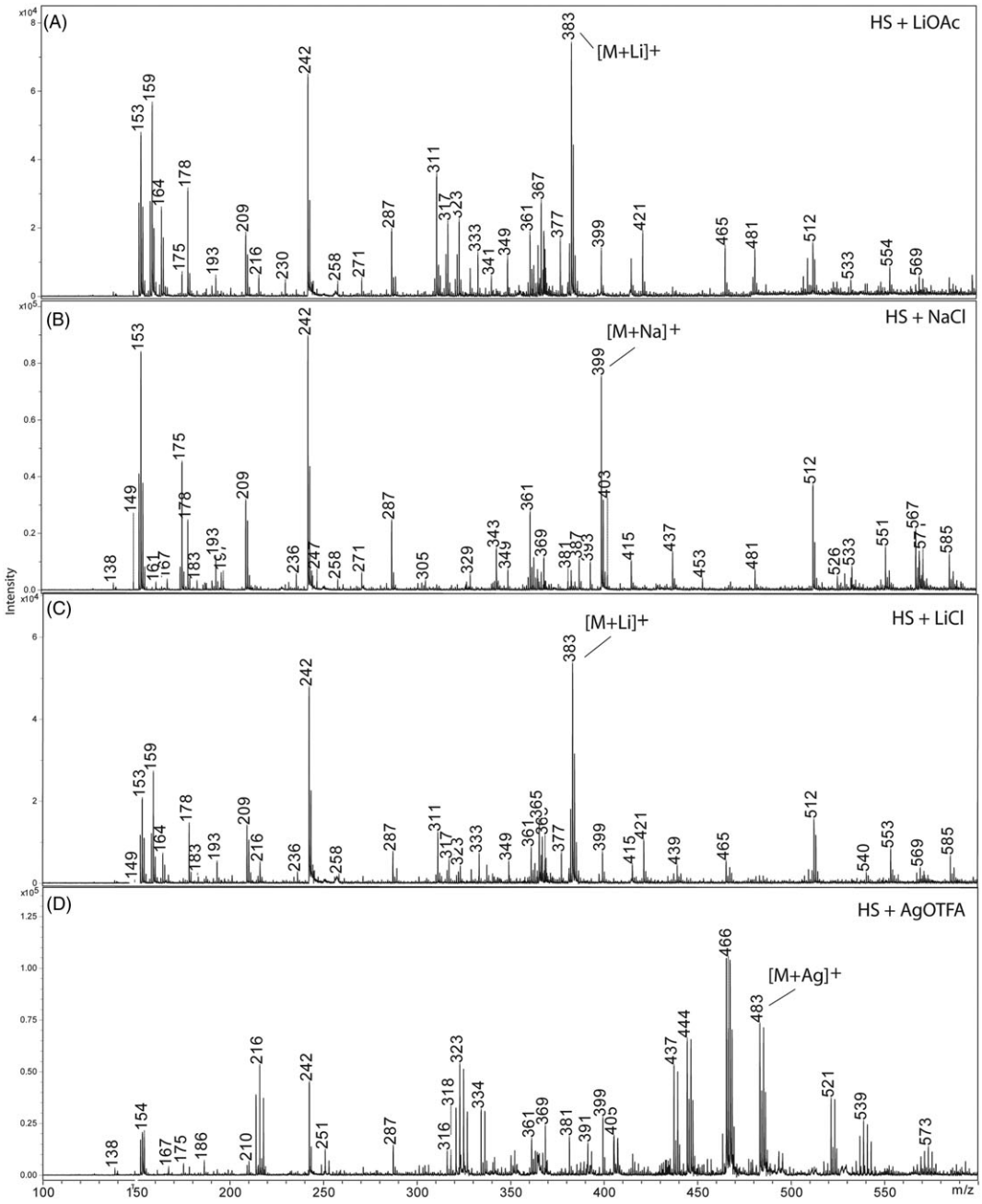

FIGURE 2 MALDI spectra of H-(β-O-4′)-S dimer analyzed with the cation sources: A, LiOAc (*m/z* 383); B, NaCl (*m/z* 399); C, LiCl (*m/z* 383); and D, $AgC_2F_3O_2$ (*m/z* 483)

due to the low analyte concentrations (0.2 mg/mL) used for these experiments. Low concentrations were utilized to provide a more "real world" example of the relative intensities to expect for each cation adduct. As noted earlier, the signals observed at *m/z* 242 were present in all samples and their presence is consistent with the tetrabutylammonium cation used in the dimer synthesis.

The lithium acetate (Figure 2A) and lithium chloride (Figure 2C) cation sources both produced adducts ions at *m/z* 383 consistent with the lithium adduct of the H-(β-O-4′)-S dimer (376 g/mol). Both spectra were similar in complexity. Using sodium chloride (Figure 2B) as the cation source produced a peak at *m/z* 399, which was consistent with the sodium adduct of the H-(β-O-4′)-S dimer. The sodium adduct spectrum contained many ions similar to those observed in the lithium adduct spectra (shifted up by 16 *m/z* units); however, the spectral intensity was greater than that obtained with lithium *vide infra*. When silver trifluoroacetate (Figure 2D) was used as the cation source, peaks at *m/z* 483 and 485 were observed originating from the silver isotopes ^{107}Ag and ^{109}Ag, respectively. The silver ion adduct spectra were quite complex and showed relatively low signal intensity; thus, silver was abandoned as a potential cation source.

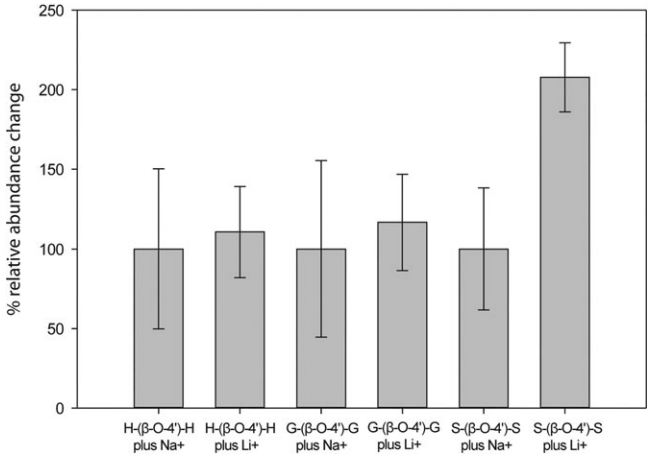

FIGURE 3 Bar graph showing the percent relative abundance increase for lithium relative to sodium cationization for three dimers, H-(β-O-4′)-H, G-(β-O-4′)-G and S-(β-O-4′)-S. Error bars indicate the %RSD for seven replicate analyses for each dimer-cation pair

3.3 | Sodium/lithium cationization comparison

In order to make a more quantitative comparison between lithium and sodium cationization, we incorporated an internal standard (HDTMA) into our MALDI analysis. Three different dimers (H-(β-O-4′)-H, G-(β-O-4′)-G and S-(β-O-4′)-S) were analyzed in the presence of HDTMA with each cation source (Li^+ and Na^+) with seven replicates each. Initial experiments determined that 10 mM was the minimum concentration required for efficient cationization of our model dimers and 1 μM of HDTMA was required to produce signal intensities similar to other ions.

To compare the cation sources directly, the ion intensity of each dimer cation adduct signal was divided by the ion intensity of the HDTMA internal standard and the resulting signal ratios for each sodium dimer adduct were normalized to 100%. Figure 3 shows the relative changes for the lithium dimer adducts relative to the sodium dimer adducts using this normalized scale.

No significant change was observed for the lithium H-(β-O-4′)-H dimer adduct compared with the sodium dimer adduct; however, the mean for the lithium dimer adduct did increase by 11% (111% ± 29% relative to the sodium dimer adduct). Again, no significant changes were observed for the lithium G-(β-O-4′)-G dimer adduct but the mean did show an increase of 17% (117% ± 30% relative to the sodium dimer adduct). In contrast the mean value for the lithium S-(β-O-4′)-S dimer adduct was significantly increased (p <0.05) by 108% (208% ± 22% relative to the sodium dimer adduct). This large increase in relative abundance for the lithium S-(β-O-4′)-S dimer adduct was attributed to the increased number of methoxy groups on this dimer which allowed lithium to achieve its stable coordination number of four.[19]

For these three dimers, the mean values indicated that lithium cationization slightly out-performed sodium cationization. The lack of statistical significance for H-(β-O-4′)-H and G-(β-O-4′)-G lithium adducts probably resulted from spotting technique issues and matrix crystal formation inherent in MALDI. The use of the internal standard improved these issues but could not overcome the variability of manual sample spotting.

3.4 | Lignin oligomer analysis

Since lithium chloride out-performed sodium chloride in terms of reproducibility and signal intensity with β-O-4' dimers, we evaluated the DHAP/Li^+ method by analyzing DHP synthesized oligomers and ferric chloride-produced synthesized oligomers as a controlled "proof of concept".

Figures 4A and 4B show a MALDI-TOF spectral comparison of the DHP-produced G oligomer and the ferric chloride produced

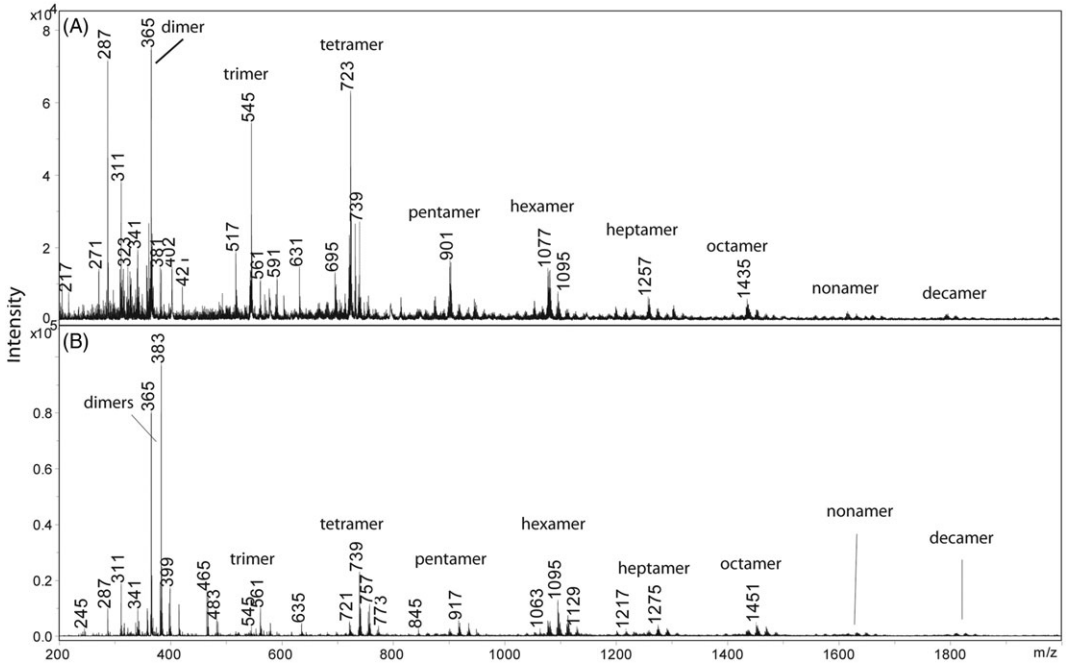

FIGURE 4 Full scan (m/z 200–2000) DHAP/Li^+ MALDI spectra of A, DHP G oligomer and B, ferric chloride G oligomer

G oligomer with LiCl in the DHAP matrix, respectively. Since G oligomers from each type contain different bonding motifs such as β-O-4', β-β' and β-5', a variety of peak clusters was observed – from dimers to decamers. Because the two G oligomers were synthesized using different reaction scenarios, the most intense signals in each cluster are not the same.

Looking at the dimer mass range, the DHP oligomer was dominated by the *m/z* 365 peak, consistent with β-β 'and/or β-5' bonding, and the β-O-4' dimer at *m/z* 383 was less than 20%, consistent with previous reports.[21,22] In contrast, the ferric chloride-produced prepared oligomers showed a significant *m/z* 383 peak, indicating a dominance of β-O-4' bonding in these oligomers. This difference in bonding selectivity can be observed at various stages of oligomerization. For example, in the tetramer region of the DHP oligomer shown in Figure 5A, we can clearly see a large *m/z* 723 peak, which is consistent with an all β-5' or a mixed β-5'/β-β' bonding. In addition, ions at *m/z* 739 and 755 correspond to replacing one and two β-β' or β-5' bonds with a β-O-4' bond, respectively. This oligomerization did not produce a peak resulting from all β-O-4' bonds. In contrast, the ferric chloride oligomerization (Figure 5B) produced a smaller peak for the all β-β' or β-5' bond oligomer at *m/z* 723 and a dominant *m/z* 739 peak, which corresponds to a trimer with two β-5' bonds and one β-O-4' bond or a trimer with a β-β', a β-5' and a β-O-4' bond. This reaction also produced an ion in the tetramer region at *m/z* 771, corresponding to two β-O-4' bonds and one β-5' bond.

To further evaluate the DHAP/Li^+ method, we synthesized a DHP co-oligomer system by simultaneously adding all three monolignols into the DHP reaction. The DHAP/Li^+ MALDI spectrum from this oligomerization is shown in Figure 6. This complex spectrum shows ions across the entire mass range. Careful inspection shows peaks containing all three monolignols. For example, the ion at *m/z* 723 was consistent with an all β-5' or a mixed β-5'/β-β' G oligomer (as shown in Figure 5A). The two ions at *m/z* 663 and 693 were consistent with the addition of two and one H monolignols, respectively.

Correspondingly, the ions at *m/z* 753 and 783 were consistent with one and two S monolignol substitutions, respectively. In addition, the observation of ions at 16 *m/z* units greater for each of these ions indicates the substitution of at least one β-O-4' bond. As the mass range increases, the separation between oligomer clusters diminished into a continuum of peaks separated by 30 *m/z* units.

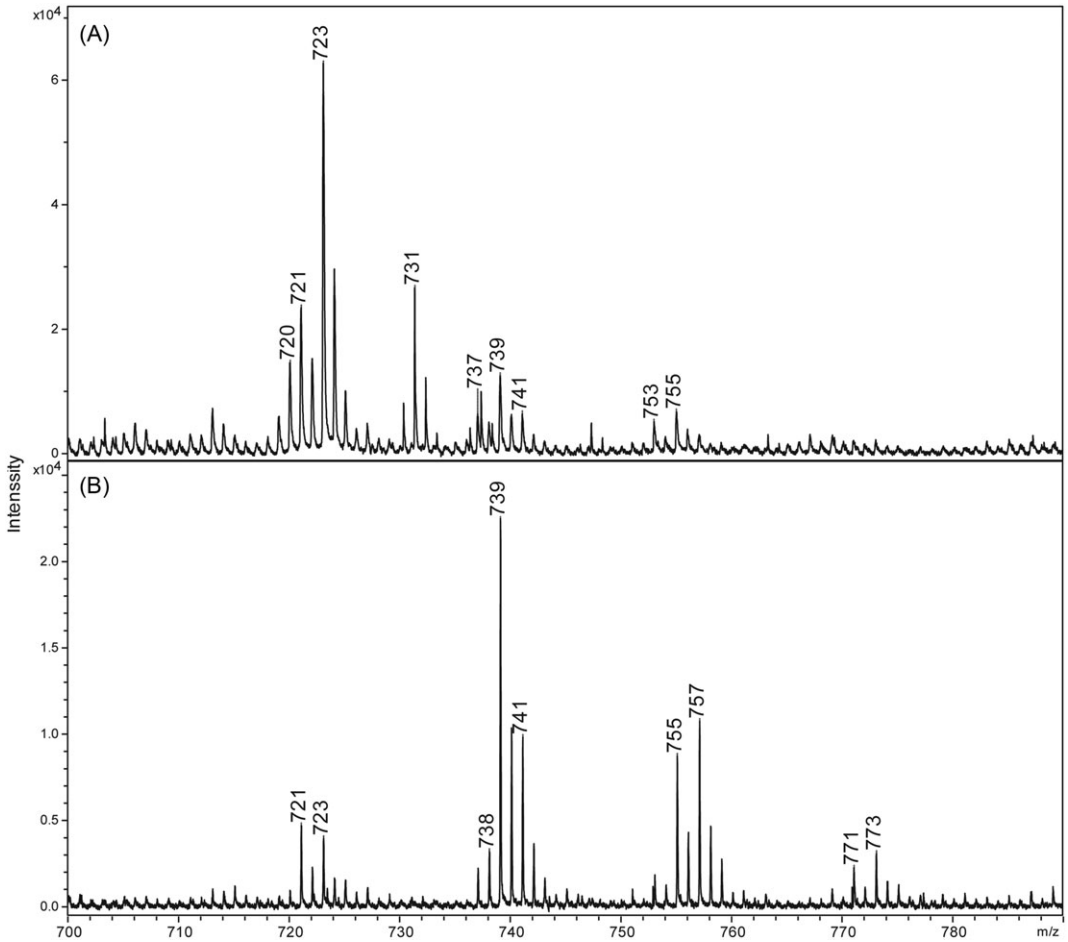

FIGURE 5 Zoomed-in view (*m/z* 700–790) of DHAP/Li^+ MALDI spectra showing the tetramer region for A, the DHP G oligomer and B, the ferric chloride G oligomer

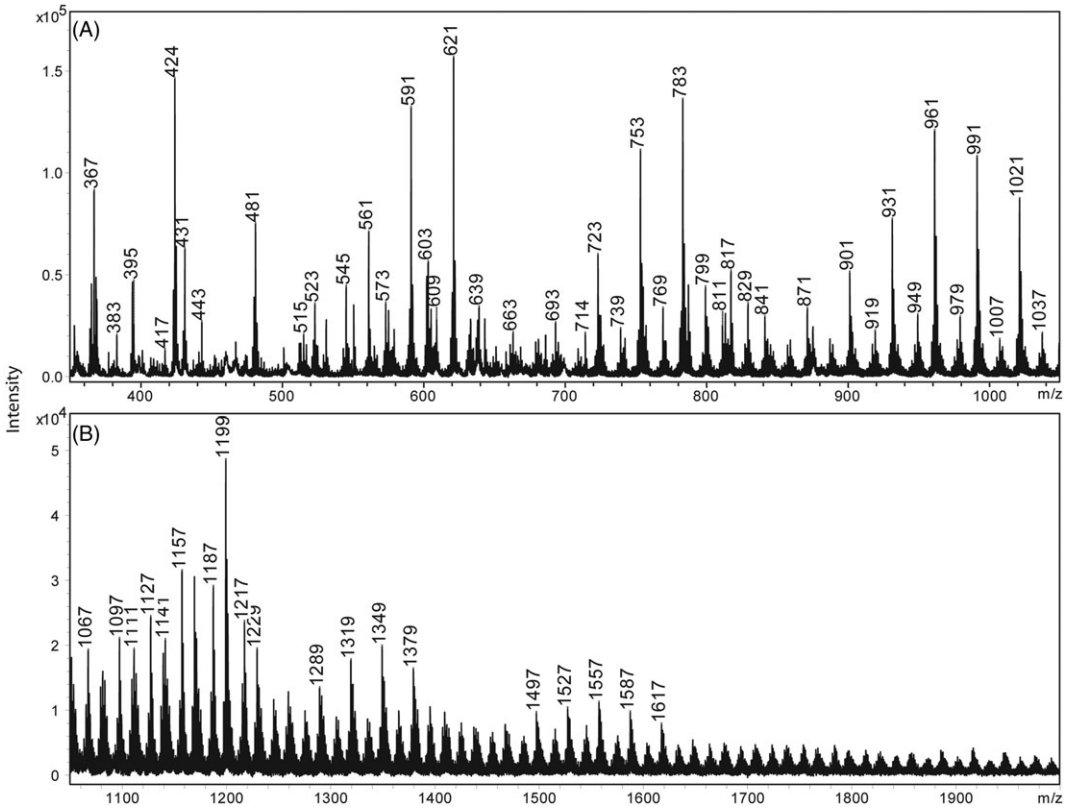

FIGURE 6 DHAP/Li^+ MALDI spectrum (*m/z* 300–2000) of a DHP copolymerized HGS system. For clarity, the mass spectrum is presented as two panels where A, shows the mass range between *m/z* 300 and 1050 and B, shows the mass range between *m/z* 1050 and 2000. A large number of features can be identified, with 30 *m/z* unit increments

4 | CONCLUSIONS

The dearth of reports utilizing MALDI-TOF-MS to study lignin and lignin degradation products does not reflect the potential usefulness of this analytical technique. Appropriate selection of a MALDI matrix with or without modifiers will ultimately resolve previously reported poor ionization and concomitant low signal intensities. Recently, Kosyakov et al reported on the use of ionic liquids as novel MALDI matrices for lignin analysis.[23] Although the MALDI spectra of their ionic liquid matrices show intense matrix-related background ions, their approach shows promise for the analysis of intact kraft and extracted lignins.

We find that the combination of the DHAP matrix and lithium cationization provides a significant increase in average signal intensity of model lignin dimers and DHP oligomers along with less complex, reproducible positive ion spectra. We are currently expanding our DHAP/Li^+ MALDI research efforts to isolated, intact lignin samples with the aim of developing a comprehensive analytical tool for the analysis of lignin oligomers.

ACKNOWLEDGEMENT

Funding for this research was provided by the National Science Foundation EPSCoR Track 2 (OIA 1632854).

ORCID

Bert C. Lynn https://orcid.org/0000-0001-8426-3024

REFERENCES

1. Forage USD, Wavre D. Lignin biosynthesis. *Annu Rev Plant Biol*. 2003;54:519-546.
2. Ragauskas AJ, Beckham GT, Biddy MJ, et al. Lignin valorization: Improving lignin processing in the biorefinery. *Science*. 2014;344:709-719.
3. Zhang Y, Liao J, Fang X, Bai F, Qiao K, Wang L. Renewable high-performance polyurethane bioplastics derived from lignin – Poly(ε-caprolactone). *Sustain Chem Eng*. 2017;5(5):4276-4284.
4. Chatterjee S, Saito T. Lignin-derived advanced carbon materials. *ChemSusChem*. 2016;8:3941-3958.
5. Cheng C, Wang J, Shen D, Xue J, Guan S, Gu S. Catalytic oxidation of lignin in solvent systems for production of renewable chemicals: A review. *Polymers*. 2017;9(240):38-50.
6. Yuan T, Sun R. Role of lignin in a biorefinery: Separation characterization and valorization. *J Chem Technol Biotechnol*. 2012;88(12):346-352.
7. Lupoi JS, Singh S, Simmons BA, Robert J. Recent innovations in analytical methods for the qualitative and quantitative assessment of lignin. *Renew Sustain Energy Rev*. 2015;49:871-906.
8. Cybulska I, Brudecki G, Rosentrater K, Julson JL, Lei H. Comparative study of Organosolv lignin extracted from prairie cordgrass, switchgrass and corn stover. *Bioresour Technol*. 2012;118:30-36.
9. Yoshioka K, Ando D, Watanabe T. A comparative study of matrix- and nano-assisted laser desorption/ionization time-of-flight mass spectrometry of isolated and synthetic lignin. *Phytochem Anal*. 2012;23(3):248-253.
10. Richel A, Vanderghem C, Simon M, Wathelet B, Paquot M. Evaluation of matrix-assisted laser desorption/ionization mass spectrometry for second-generation lignin analysis. *Anal Chem Insights*. 2012;7(1):79-89.

11. De Angelis F, Fregonese P, Veri F. Structural investigation of synthetic lignins by matrix-assisted laser desorption/ionization time-of-flight mass spectrometry. *Rapid Commun Mass Spectrom*. 1996;10(6):1304-1308.
12. Penno M, Ernst M, Hoffmann P. Optimal preparation methods for automated matrix-assisted laser desorption/ionization time-of-flight mass spectrometry profiling of low molecular weight proteins and peptides. *Rapid Commun Mass Spectrom*. 2009;23(17):2656-2662.
13. Wenzel T, Sparbier K, Mieruch T, Kostrzewa M. 2,5-Dihydroxyacetophenone: A matrix for highly sensitive matrix-assisted laser desorption/ionization time-of-flight mass spectrometric analysis of proteins using manual and automated preparation techniques. *Rapid Commun Mass Spectrom*. 2006;20(5):785-789.
14. Hayasaka T, Goto-Inoue N, Masaki N, Ikegami K, Setou M. Application of 2,5-dihydroxyacetophenone with sublimation provides efficient ionization of lipid species by atmospheric pressure matrix-assisted laser desorption/ionization imaging mass spectrometry. *Surf Interface Anal*. 2014;46(12-13):1219-1222.
15. Jovanovic M, Peter-Katalinic J. Negative ion MALDI-TOF MS, ISD and PSD of neutral underivatized oligosaccharides without anionic dopant strategies, using 2,5-DHAP as a matrix. *J Mass Spectrom*. 2016;51(2):111-122.
16. Hoberg AM, Haddleton DM, Derrick PJ. Updating evidence for cationization of polymers in the gas phase during matrix-assisted laser desorption/ionization. *Eur Mass Spectrom*. 2005;3(6):471-473.
17. Hernandez O, Isenberg S, Steinmetz V, Glish GL, Maitre P. Probing mobility-selected saccharide isomers: Selective ion-molecule reactions and wavelength-specific IR activation. *J Phys Chem A*. 2015;119(23):6057-6064.
18. Asare SO, Huang F, Lynn BC. Characterization and sequencing of lithium cationized β-O-4 lignin oligomers using higher-energy collisional dissociation mass spectrometry. *Anal Chim Acta*. 2019;1047:104-114.
19. Olsher U, Izatt RM, Bradshaw JS, Dalley NK. Coordination chemistry of lithium ion: A crystal and molecular structure review. *Chem Rev*. 1991;91(2):137-164.
20. Asare SO, Kamali P, Huang F, Lynn BC. Application of chloride adduct ionization tandem mass spectrometry for characterizing and sequencing synthetic lignin model compounds. *Energy Fuel*. 2018;32(5):5990-5998.
21. Ralph J, Lundquist K, Brunow G, et al. Lignins: Natural polymers from oxidative coupling of 4-hydroxyphenylpropanoids. *Photochem Rev*. 2004;3(1-2):29-60.
22. Méchin V, Baumberger S, Pollet B, Lapierre C. Peroxidase activity can dictate the *in vitro* lignin dehydrogenative polymer structure. *Photochemistry*. 2007;68(4):571-579.
23. Kosyakov D, Anikeenko1 EA, Ul'yanovskii1 NV, Khoroshev OU, Shavrina1 IS, Gorbova NS. Ionic liquid matrices for MALDI mass spectrometry of lignin. *Anal Bioanal Chem*. 2018;410(28):7429-7439.

How to cite this article: Bowman AS, Asare SO, Lynn BC. Matrix-assisted laser desorption/ionization time-of-flight mass spectrometry analysis for characterization of lignin oligomers using cationization techniques and 2,5-dihydroxyacetophenone (DHAP) matrix. *Rapid Commun Mass Spectrom*. 2019;33:811–819. https://doi.org/10.1002/rcm.8406